





Article

Application of New Efficient Hoveyda–Grubbs Catalysts Comprising an N→Ru Coordinate Bond in a Six-Membered Ring for the Synthesis of Natural Product-Like Cyclopenta[*b*]furo[2,3-*c*]pyrroles

Alexandra S. Antonova ¹, Marina A. Vinokurova ¹, Pavel A. Kumandin ¹, Natalia L. Merkulova ¹, Anna A. Sinelshchikova ² , Mikhail S. Grigoriev ² , Roman A. Novikov ³, Vladimir V. Kouznetsov ⁴ , Kirill B. Polyanskiy ^{1,*} and Fedor I. Zubkov ^{1,*} 

¹ Organic Chemistry Department, Faculty of Science, Peoples' Friendship University of Russia (RUDN University), Miklukho-Maklaya St., 6, 117198 Moscow, Russia; alexandrasantonova@gmail.com (A.S.A.); marina.vin1999@yandex.ru (M.A.V.); pakumandin@gmail.com (P.A.K.); fraumerk@gmail.com (N.L.M.)

² A. N. Frumkin Institute of Physical Chemistry and Electrochemistry, Russian Academy of Sciences, Leninsky pr. 31, bld. 4, 119071 Moscow, Russia; asinelshchikova@gmail.com (A.A.S.); mickgrig@mail.ru (M.S.G.)

³ V. A. Engelhardt Institute of Molecular Biology, Russian Academy of Sciences, Vavilov Street, 32, 119991 Moscow, Russia; novikovfff@bk.ru

⁴ Laboratorio de Química Orgánica y Biomolecular, CMN, Universidad Industrial de Santander, Parque Tecnológico Guatiguara, Km 2 vía refugio, Piedecuesta A.A. 681011, Colombia; kouznet@uis.edu.co

* Correspondence: 1236tgp@mail.ru (K.B.P.); fzubkov@sci.pfu.edu.ru (F.I.Z.); Tel./Fax: +7-(495)-952-26-44 (F.I.Z.)

Academic Editors: Igor V. Trushkov and Maxim G. Uchuskin

Received: 3 November 2020; Accepted: 14 November 2020; Published: 17 November 2020



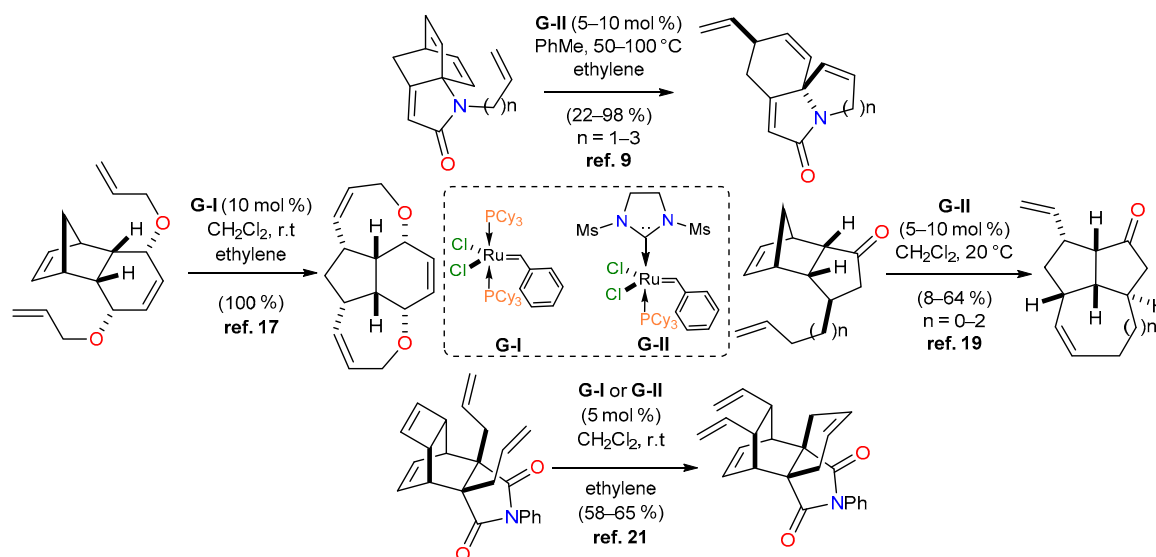
Abstract: The ring rearrangement metathesis (RRM) of a *trans-cis* diastereomer mixture of methyl 3-allyl-3a,6-epoxyisindole-7-carboxylates derived from cheap, accessible and renewable furan-based precursors in the presence of a new class of Hoveyda–Grubbs-type catalysts, comprising an N→Ru coordinate bond in a six-membered ring, results in the difficult-to-obtain natural product-like cyclopenta[*b*]furo[2,3-*c*]pyrroles. In this process, only one diastereomer with a *trans*-arrangement of the 3-allyl fragment relative to the 3a,6-epoxy bridge enters into the rearrangement, while the *cis*-isomers polymerize almost completely under the same conditions. The tested catalysts are active in the temperature range from 60 to 120 °C at a concentration of 0.5 mol % and provide better yields of the target tricycles compared to the most popular commercially available second-generation Hoveyda–Grubbs catalyst. The diastereoselectivity of the intramolecular Diels–Alder reaction furan (IMDAF) reaction between starting 1-(furan-2-yl)but-3-en-1-amines and maleic anhydride, leading to 3a,6-epoxyisindole-7-carboxylates, was studied as well.

Keywords: furan; Hoveyda–Grubbs catalysts; nitrogen–ruthenium coordinate bond; ring-rearrangement metathesis; cyclopenta[*b*]furo[2,3-*c*]pyrroles; 3-allyl-3a,6-epoxyisindoles; IMDAF reaction

1. Introduction

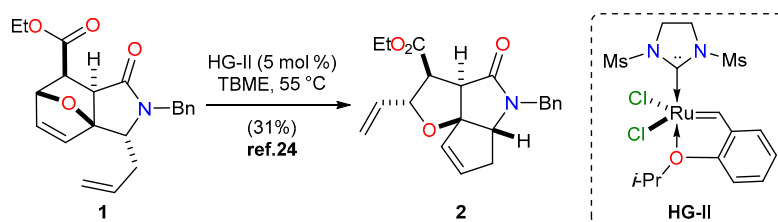
The discovery of metathesis reactions has allowed the noticeable expansion of possibilities for the transformation of different unsaturated substrates, including those aimed at obtaining complex naturally occurring compounds and pharmacologically meaningful molecules, which is reflected in a number of recent reviews [1–8]. In particular, the ring-rearrangement metathesis (RRM) of bi- and polycyclic alkenes has made it possible to obtain systems that are practically inaccessible by

means of other synthetic pathways [9–18]. Most often, for the rearrangement of bridged alkenes, the commercially available Grubbs (G) and Hoveyda–Grubbs (HG) ruthenium catalysts are used, which permits the reliable production of scaffolds possessing a wide range of potential biological activity due to the characteristics of their carbon skeletons [19–23]. Representative examples of the above-mentioned metathesis reactions clearly demonstrate a variety of possible transformation routes that give the structural diversity of the available final products (Scheme 1). As can be seen, the direction of the reaction may depend not only on the structure of the substrate, but also on the reaction conditions selected and the chosen catalyst.



Scheme 1. Selected examples of the ring-rearrangement metathesis (RRM) of tri- and tetracyclic bridged systems closest to the topic of this study.

Moreover, among all the variety of metathesis products known to date, there is a sole successful example of the HG-catalyzed RRM of 3a,6-epoxyisondole **1** which has produced the previously unknown heterocyclic system of cyclopenta[*b*]furo[2,3-*c*]pyrrole **2**, but in modest yield (31%) [24] (Scheme 2).



Scheme 2. Synthesis of cyclopenta[*b*]furo[2,3-*c*]pyrrole core **2** via ring-rearrangement metathesis (HG-II—the second-generation Hoveyda–Grubbs catalyst, TBME—methyl *tert*-butyl ether) [24].

Hence, further investigations of the influence of catalysts and the structure of unsaturated substrates on the selectivity of metathesis reactions remain an ongoing trend in modern organic synthesis. The selection of main starting materials for the suitable unsaturated substrates like **1** is also an important task. In this context, it should be noted that the starting material for **1** is furfural, which is a renewable chemical and one of the most available agricultural byproducts from biomass [25,26]. In regard to design of new catalysts for RRM, our group recently prepared a new class of effective ruthenium catalysts comprising an N→Ru coordinate bond in a six-membered ring (**Cat.1** and **Cat.2**) (Figure 1) and found that they revealed a high level of activity (up to 10^{−2} mol%) in standard

models for the olefin metathesis (styrene, allylbenzene, diethyl diallylmalonate, diallyltosylamide, norbornen/hex-1-ene, etc.) [27,28].

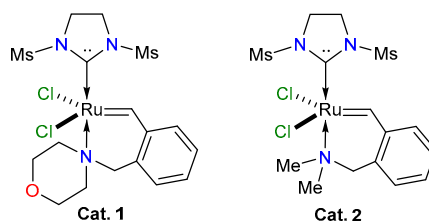
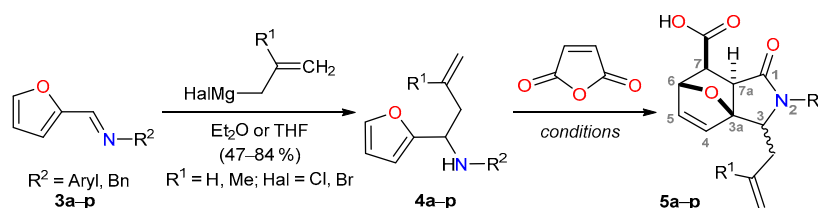


Figure 1. Hoveyda–Grubbs-type catalysts [27] used for metathesis reactions in the present work.

According to the statements above and with the knowledge that there are no reports on the efficient synthetic methods for diversely polyfunctionalized cyclopenta[*b*]furo[2,3-*c*]pyrroles using easily available 3-allyl-3a,6-epoxyisoindoles derived from 1-(furan-2-yl)-*N*-arylmethanimines through the intramolecular Diels–Alder furan (IMDAF) reaction, our research was focused on: (i) Establishing the optimal conditions for the diastereoselective preparation of 3-allyl-3a,6-epoxyisoindoles, according to the variables: solvent, acid catalysts, reaction time and temperature; (ii) With the determined conditions in hand, preparing diverse 3a,6-epoxyisondol-7-carboxylic acids and their methyl esters; (iii) Corroborating the spatial structure of isomeric acids and their esters; (iv) Studying the catalytic activity of ruthenium catalysts **1** and **2** in the RRM of 3a,6-epoxyisoindole-7-carboxylates in comparison with HG-II catalyst; and (v) With the established conditions in hand, preparing the desired cyclopenta[*b*]furo[2,3-*c*]pyrroles. All this is in order to develop new, short and efficient synthesis of natural product-like scaffolds from renewable furan-based precursors.

2. Results and Discussion

The principal synthetic scheme for the required 3-allyl-3a,6-epoxyisoindole-7-carboxylic acids **5** preparation includes two key steps and is based on readily available starting materials. The condensation of aryl amines (or benzyl amines) and furfural gives the corresponding Schiff bases **3**, which, being treated with Grignard reagents (allyl magnesium bromide or methallyl magnesium chloride), give rise to homoallylamines **4** in multigram quantities (Scheme 3) [29–32].



Scheme 3. Synthesis of the starting 3a,6-epoxyisoindole-7-carboxylic acids **5** [29–32].

The subsequent reaction of furfurylamines **4** with maleic anhydride easily provides the corresponding isoindolocarboxylic acids **5**, which were isolated in good overall yields. The IMDAF reaction is highly stereoselective [33,34]; in the course of the tandem *N*-acylation/[4+2] cycloaddition sequence, only *exo*-adducts form as a mixture of two diastereomers (*trans*-**5A** and *cis*-**5B**) based on the orientation of the 3-allyl (or 3-methallyl) substituent relative to the 3a,6-epoxy-bridge (Figure 2).

As we showed earlier [29–32], the synthesized 3-allyl-3a,6-epoxyisoindole-7-carboxylic acids **5** are excellent precursors for heterocyclization into the corresponding isoindoloquinolines and isoindolobenzazepines. In this process, the isomeric composition of adducts **5A/5B** had no strong influence on the yield and stereochemistry of the target heterocycles. In contrast, as was demonstrated in the first experiments in this study, only derivatives of the *trans*-isomer **5A** are capable of further

transformation under RRM conditions. Thus, in the second stage of this investigation, we tried to resolve the problem of the diastereoselectivity of the IMDAF reaction.

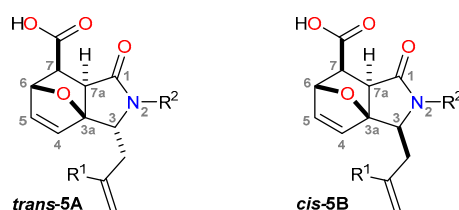


Figure 2. Structures of the *cis* and *trans* diastereoisomers of 3a,6-epoxyisoindole-7-carboxylic acids **5**.

Considering the fact that reversible Diels–Alder reactions are most influenced by the reaction temperature and the polarity of the solvent [35–38], we compared the isomeric composition of the most diverse acids **5a,b,g,i,m** formed under the conditions indicated in Table 1. The application of Lewis acids (10–25 mol % of AlEt₃, BF₃·OEt₂, TiCl₄) as catalysts in MeCN, PhH, PhMe, or CH₂Cl₂ turned out to be ineffective, probably due to their fast binding by a free carboxyl group of the products and due to the difficulties associated with the purification of the resulting reaction mixtures. Without catalyst addition, the pure target products precipitated from all tested solvents after the period of reaction time indicated in Table 1, wherein acetonitrile showed the worst results both at room and at elevated temperatures, apparently due to the partial dissolution of the target acids. As a result, it was found that according to ¹H-NMR analysis, the *cis*-isomer **B**, inactive in the metathesis reaction, mainly forms at r.t in CH₂Cl₂ (average predominance 92%), while the desired *trans*-isomer **A** is mainly produced at –16 °C in the same solvent (average predominance 68%).

Table 1. Influence of solvents and temperature on the yields and ratios of *trans*-**5A**/*cis*-**5B** isomers of 3-allyl-1-oxo-3a,6-epoxyisoindole-7-carboxylic acids (**5**).

Compd.	Substituents		Conditions, Ratios of <i>Trans</i> - 5A / <i>cis</i> - 5B Isomers ^a , and Total Yields (%)						
	R ¹	R ²	CH ₂ Cl ₂ –16 °C, 3 d	CH ₂ Cl ₂ r.t, 3 d	MeCN r.t, 3 d	MeCN Δ, 3 h	PhH Δ, 3 h	PhMe r.t, 3 d	PhMe Δ, 3 h
5a	H	Ph	76/24 (43)	7/93 (58)	47/53 (45)	44/56 (15)	59/41 (82)	48/52 (85)	59/41 (90)
5b	H	3-MeC ₆ H ₄	63/37 (49)	6/94 (65)	59/44 (41)	52/48 (25)	58/42 (85)	55/45 (90)	57/43 (92)
5g	H	4-IC ₆ H ₄	75/25 (52)	0/100 (67)	24/75 (38)	28/72 (23)	52/48 (86)	78/22 (90)	71/29 (91)
5i	Me	Ph	68/32 (63)	23/77 (75)	53/47 (62)	50/50 (47)	59/41 (95)	67/33 (97)	67/33 (98)
5m	Me	Bn	60/40 (64)	4/96 (77)	55/45 (65)	58/42 (54)	59/41 (96)	59/41 (98)	56/44 (99)
Average values			68/32 (54)	8/92 (68)	48/52 (50)	46/54 (33)	57/43 (89)	61/39 (92)	62/38 (94)

^a The ratios of the *trans*-**5A**/*cis*-**5B** isomers were established by ¹H-NMR analysis of the isolated solids.

Decreasing the temperature to below –30 °C sharply slowed down the rate of interaction between maleic anhydride and secondary amines **4**; however, at the same time, analysis of the data in Table 1 shows that the yields of the isomer **5A/5B** mixtures obtained in CH₂Cl₂ are 1.5–2 times lower compared to the mixtures isolated from benzene or toluene. Besides, the last two solvents provide a slight predominance of the isomer **5A** at both r.t and heating. It is also important to note that the reaction time was the shortest in boiling toluene (~1 h); nevertheless, for a reasonable comparison of the results in Table 1, all reactions were carried out in boiling solvents for 3 h. Thus, for further experiments, we synthesized mixtures of the *trans*-**5A**/*cis*-**5B** isomers either in dichloromethane at –16 °C or in PhMe at 3 h reflux, as indicated in Table 2.

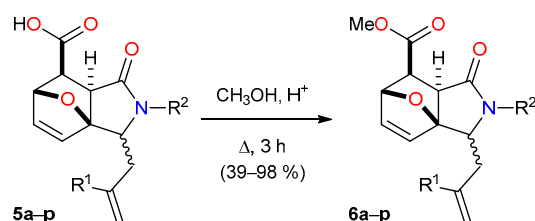
Table 2. Substituents R, isomer ratios, and yields for compounds 5–7.

Entry	R ¹	R ²	<i>Trans</i> -5A/ <i>Cis</i> -5B Ratio	Yield of Acid 5, %	<i>Trans</i> -6A/ <i>Cis</i> -6B Ratio	Yield of Ester 6, %	Yield of Tricycle 7, %
a	H	Ph	76/24	90 ^b	79/21	85	68 ^c
					95/5 ^e	53 ^e	83 ^c
					2/98 ^c	12 ^e	0 ^c
b	H	3-MeC ₆ H ₄	57/43	95 ^a	69/31	63	57 ^c
c	H	Bn	90/10	57 ^b	85/15	85	65 ^c
d	H	3-ClC ₆ H ₄	76/24	48 ^b	70/30	80	57 ^c
e	H	4-ClC ₆ H ₄	80/20	91 ^a	70/30	72	73 ^c
					98/2 ^e	46 ^e	89 ^c
					8/92 ^c	18 ^e	0 ^c
f	H	4-BrC ₆ H ₄	80/20	92 ^a	72/28	70	63 ^c
					99/1 ^e	46 ^e	87 ^c
					5/95 ^c	12 ^e	0 ^c
g	H	4-IC ₆ H ₄	71/29	52 ^b	59/41	63	48 ^c
h	H	3-Cl,4-FC ₆ H ₃	57/43	90 ^a	66/34	86	54 ^c
i	Me	Ph	68/32	63 ^b	55/45	53	50 ^d
j	Me	3-MeC ₆ H ₄	60/40	67 ^b	45/55	73	38 ^d
k	Me	4-MeC ₆ H ₄	51/49	93 ^a	50/50	98	44 ^d
l	Me	4- <i>i</i> PrC ₆ H ₄	71/29	88 ^a	87/13	82	62 ^d
m	Me	Bn	56/44	64 ^a	42/58	57	39 ^d
n	Me	2-ClC ₆ H ₄	71/29	63 ^b	75/25	95	59 ^d
o	Me	3-ClC ₆ H ₄	68/32	69 ^b	83/17	78	61 ^d
p	Me	4-BrC ₆ H ₄	76/24	64 ^b	57/43	56	52 ^d
					65/35 ^e	45 ^e	61 ^d

Conditions: ^a PhMe, Δ, 3 h; ^b **Cat.1**, CH₂Cl₂, −16 °C, 3 d; ^c **Cat.2**, CHCl₃, Δ, 30 min, under argon; ^d CH₂Cl₂, MW, 120 °C, 10 min, under argon; ^e In light grey—ratios and yields are presented after separation of the above indicated isomer 6A/6B mixture (in dark gray) with methanol.

The third part of the work is related to the study of the catalytic activity of ruthenium catalysts **1** and **2** (Figure 1) under the RRM protocol. According to the previous paper [27], the *N,N*-dimethyl catalyst **2** is the most thermally stable, while the morpholine derivative catalyst **1** is the most active (as it has the longest coordination N→Ru bond ~2.32 Å).

With this in mind, only two of these complexes were selected for the present study. The direct introduction of acids **5** into the RRM was obviously impossible due to their poor solubility in common organic solvents and due to the presence of a free carboxylic group in their structure, which is destructive to Hoveyda–Grubbs catalysts. Thus, methyl esters **6** of corresponding acids **5** were prepared according to the classical procedure (Scheme 4, Table 2).



Scheme 4. Esterification of 3a,6-epoxyindol-7-carboxylic acids **5** with methanol affording respective 3a,6-epoxyindole-7-carboxylates (**6**).

As the entries **a**, **h**, **k**, **n** in Table 2 reveal, the *trans/cis* isomeric ratio of acids **5** does not change noticeably during the esterification process, i.e., retro-DA reaction or epimerization do not proceed under selected conditions. Esters **6** obtained in this way are crystalline, easily isolated substances that are readily soluble in dichloromethane.

Elucidation of the spatial structure of isomeric acids similar to **5A/5B** and esters similar to **6A/6B** has been previously done in the literature more than once [29–32,37,39–42], while as a rule, 2D NOE NMR data have been used for evidence of their structures. Here we present X-ray structural information for a pair of isomeric methyl esters **6eA/6eB**, which confirms the preceding conclusions concerning the location of the substituent in the third position of the heterocyclic core (Figure 3).

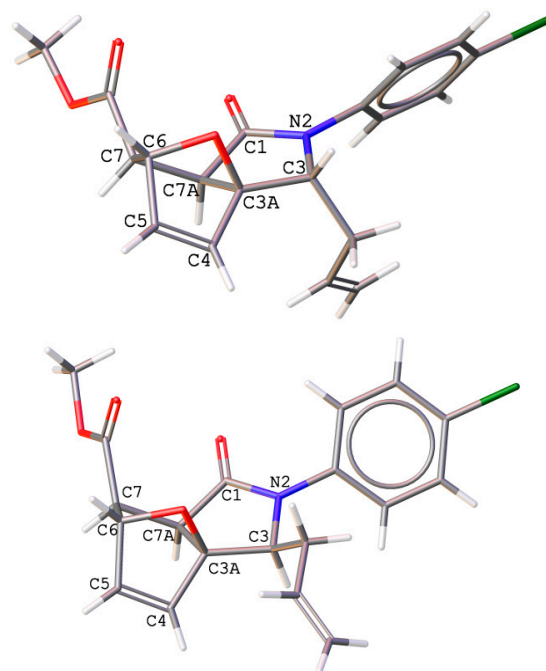


Figure 3. X-ray crystal structures of *trans*-**6eA** (at the **top**) and *cis*-**6eB** (at the **bottom**) methyl 3-allyl-2-(4-chlorophenyl)-1-oxo-1,2,3,6,7,7a-hexahydro-3a,6-epoxyisoindole-7-carboxylates.

Single crystals of diastereoisomers **6e** were grown from an ether solution, and single-crystal XRD analysis revealed that both isomers comprised 3a,6-epoxyisoindolo-7-carboxylates with one molecule in an asymmetric unit. *Trans*-**6eA** isomer crystallizes in the triclinic crystal system P-1 space group, while the *cis*-**6eB** isomer crystallizes in the orthorhombic crystal system P2₁2₁2₁ space group. The configuration of the tricyclic system is identical for both isomers (see Tables S2–S6 for bond lengths and angles, and Figure S1 for the overlay of the two molecules). The substituents in the third position of the heterocyclic core are located in *trans* or *cis* positions that influence the distance between atoms, which are key for an NOE analysis (Table 3). The phenyl rings of 3a,6-epoxyisoindolo-7-carboxylates are twisted at different angles with respect to the heterocycle due to the different orientations of the bulky substituent in the third position. In the case of *cis*-isomer **6eB**, the angle between the C₆ plane of phenyl atoms and the C(1)N(2)C(3) plane is equal to 44°, while for *trans*-isomer **6eA**, this angle is 125°. The orientation of the methyl esters group differs only slightly for both isomers (Figure 3).

Table 3. Selected interatomic distances (Å) in esters **6eA** and **6eB** according to single-crystal XRD.

Distances (Å)	<i>Trans</i> - 6eA	<i>Cis</i> - 6eB
H(3) ⋯ H(7a)	3.781(1)	2.915(1)
H(3) ⋯ H(4)	3.493(1)	2.871(1)
C(10) ^a ⋯ H(4)	4.521(2)	3.772(5)

^a C(10) is the methylene carbon atom of the allyl fragment.

The indicated X-ray parameters (for **6eA** and **6eB**) are in good agreement with the data from 2D NOESY NMR experiments carried out for *trans*- and *cis*-isomers of compounds **5e,k,m,p** and **6e,k,m,p** (**A/B**) (Figure 4).

All these compounds have a similar configuration of the tricyclic skeleton and side groups for different substituents and gave the same cross-peaks in the NOESY spectra. Key NOE interactions are indicated in Figure 4. There are strong NOE interactions between H(4)–H(7a) and H(5)–H(7) for both diastereomers, indicating their identical endo-configurations for protons H(7) and H(7a). The difference lies in the side allyl/methylallyl group, which is present in *trans*- or *cis*-form. There are

strong resulting cross-peaks in the NOESY spectra between H(4)–H2C for *trans*-diastereomer **A** and H(4)–H(3) and H(3)–H(7a) for *cis*-diastereomer **B** (green arrows in Figure 4), which indicates their spatial proximity (<3 Å) and fully corresponds to the XRD data (Table 3). Cross-peaks between these protons but for other diastereomers (**B** and **A**, respectively)—between H(4)–H(3) and H(3)–H(7a) for *trans*-diastereomer **A** and H(4)–H2C for *cis*-diastereomer **B**—are absent in the NOESY spectra almost completely (crossed-out red arrows in Figure 4). The side allyl/methallyl group is conformationally quite mobile in solution, and NOE data for it cannot be appropriately compared with XRD distances.

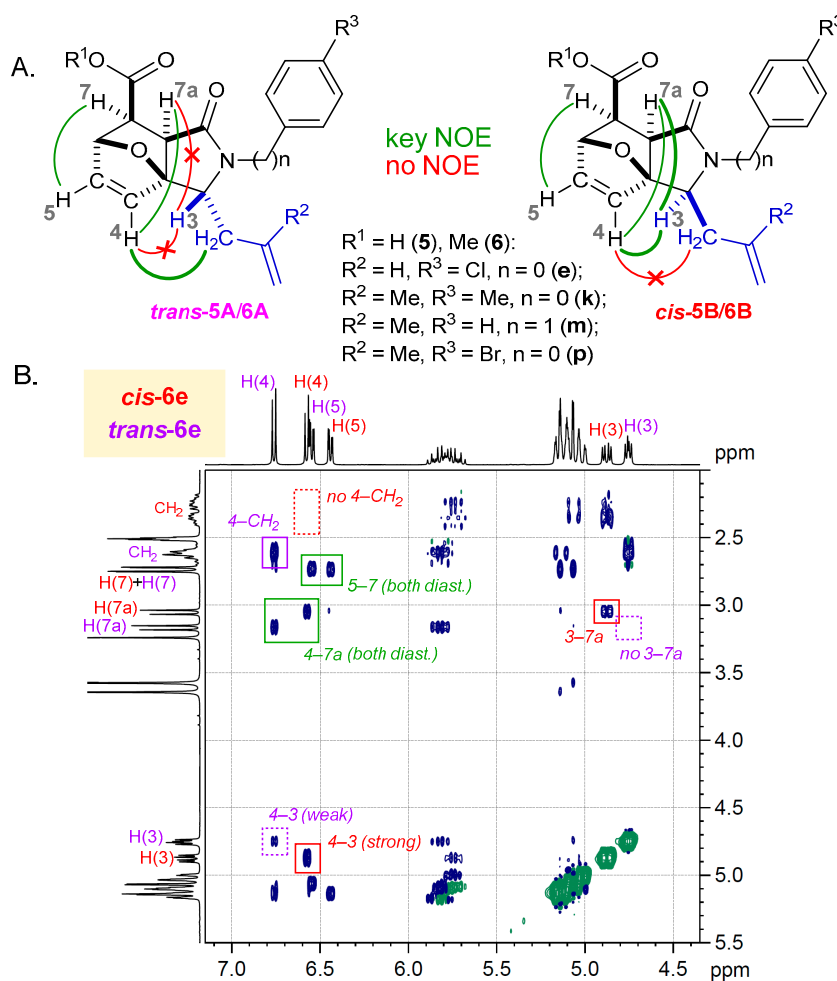


Figure 4. (A.) Key observed NOE interactions in 2D NOESY NMR spectra for both representative *trans*- and *cis*-diastereomers **5e,k,m,p** and **6e,k,m,p** (A/B). (B.) Representative part of 2D NOESY spectra for mixture of *trans*- (violet) and *cis*- (red) diastereomers of the allyl derivative **6e** with assignments of signals and NOE.

¹H and ¹³C-NMR spectra for series **5/6** of *trans*- and *cis*-diastereomers **A/B** have very few characteristic signals by which they could be easily distinguished. However, they have several characteristic patterns of correlation peaks in 2D HSQC spectra (Figure 5 and see the ESI with assignments data), for example, for CH(4) and CH(5) alkene protons, *ortho*-CH/*meta*-CH for *para*-substituted aromatics at N(2), and aliphatic CH₂-groups in allyl/methallyl fragment. In the whole, the absolute values of chemical shifts are non-characteristic, since there is a fairly large scatter of chemical shifts depending on the substituents. However, for a number of protons and carbons, the sequence of the signals and difference of their chemical shifts are characteristic and the same for all compounds. The H(3), H(4), H(7a), CH₂ protons, and the CH(3), C(3a), CH₂ carbons have such features. Data on them are given in Tables S12 and S13 (see the ESI).

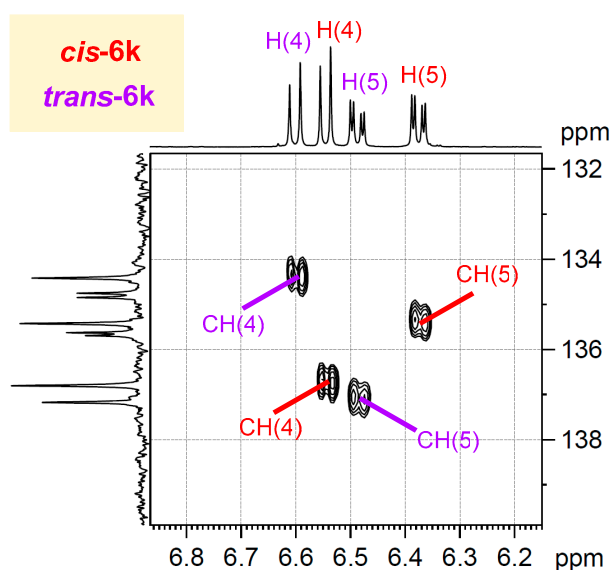
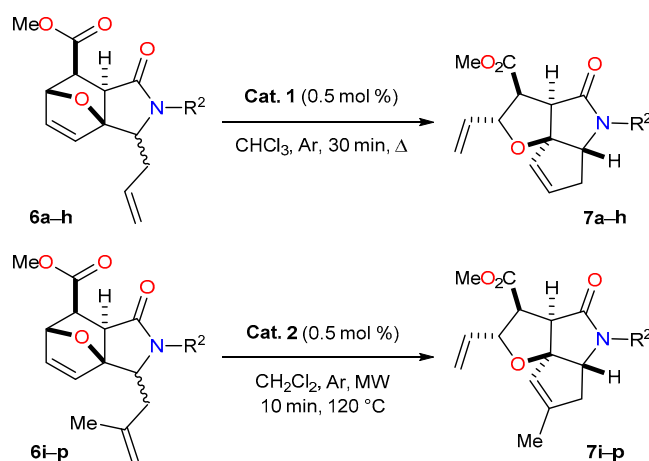
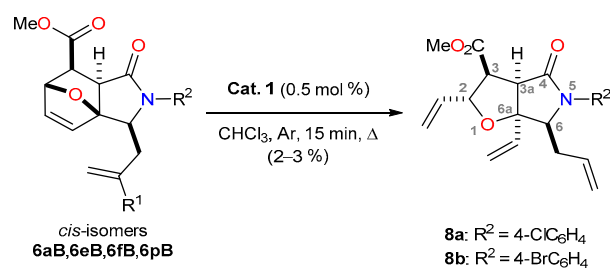


Figure 5. Typical characteristic pattern of CH(4) and CH(5) correlation peaks in 2D HSQC spectra (mixture of trans and cis diastereomers of **6k** as an example) used for assignments of diastereomers.

Therefore, the combination of the single-crystal XRD and NMR data allowed us to make an unambiguous assignment of isomers of all compounds **5** and **6** to the **A** or **B** series.

Considering that we were unable to achieve a noticeable predominance of the desired acids **5A** by varying the IMDAF reaction conditions (see Table 1), we paid close attention to finding preparative methods for the separation of isomeric esters **6A/6B**. We failed to find a suitable chromatographic system for the separation of isomers **6A/6B** on silica gel due to the closeness of their retention factors. Mixtures of diastereomers **6aA/6aB** (79/21), **6eA/6eB** (16/84), **6fA/6fB** (29/71) and **6pA/6pB** (57/43) were used as model compounds, and mixtures of EtOAc/hexane, MeOH/THF and CHCl₃/MeOH were applied as eluents. However, our attempts to separate the same esters by fractional crystallization were more fruitful. For this purpose, fine powders of the stereoisomer mixtures were stirred for a half-hour at 45–50 °C in a methanol solution; then, the least soluble isomer **6B** was filtered off and the mother liquor was concentrated. After this treatment, the purity of individual isomers **6A** and **6B** exceeded 92% (diastereomeric excess (*de*) > 84%) in total yields of more than 94%. Repeating this procedure one more time resulted in virtually pure isomers. According to the described protocol, the diastereomers of 3-allyl substituted esters **6aA/6aB**, **6fA/6fB** and **6eA/6eB** were separated and tested as metathesis objects (Scheme 5), described in the third part of this manuscript. Separation of 3-methallyl substituted esters **6pA/6pB** by this way was less efficient, resulting in the formation of a 65/35 mixture of isomers after one “recrystallization” from MeOH.

The first experiments showed that solutions of the individual *cis*-isomers **6aB**, **6eB** and **6fB** in CH₂Cl₂ at both room and elevated temperatures underwent polymerization with catalysts **1**, **2** or HG-II (0.5–5 mol%). We were unable to isolate individual substances from metathesis product mixtures obtained under either an argon or an ethylene atmosphere (2 bar), except in two cases **6eB** (R¹ = H, R² = 4-ClC₆H₄) and **6fB** (R¹ = H, R² = 4-BrC₆H₄). In these tests under an argon atmosphere, divinyl furo[2,3-*c*]pyrroles **8**, probably the products of a series of the sequenced intermolecular cross metathesis reactions, were localized in a very low yield (Scheme 6). The formation of this product only occurs if the reaction is carried out for 15 min or less; upon longer heating, products **8** are completely transformed into a polymer.

Scheme 5. Synthesis of cyclopenta[*b*]furo[2,3-*c*]pyrroles 7.Scheme 6. Results of metathesis of *cis*-isomers **6B**.

In these two cases, it turned out to be possible to isolate products using column chromatography. The spatial structure of one of them (**8b**) was entirely confirmed by X-ray analysis (Figure 6). Compounds **8a** and **8b** also can be obtained by reaction of the esters **6e** or **6f** with ethylene (2 bar, 100 °C, 6 h) in dichloromethane in presence of catalyst **2** in 5–8% yields.

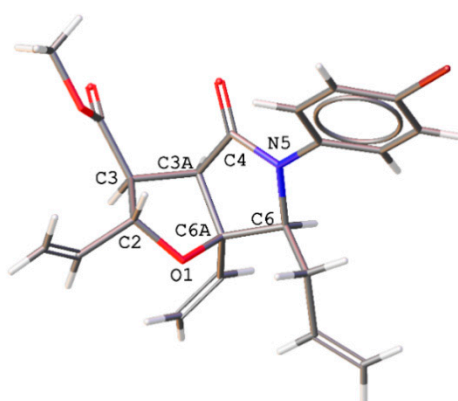


Figure 6. X-ray crystal structure of methyl (2*RS*,3*SR*,3*aRS*,6*SR*,6*aSR*)-6-allyl-5-(4-bromophenyl)-4-oxo-2,6*a*-divinylhexahydro-2*H*-furo[2,3-*c*]pyrrole-3-carboxylate (**8b**).

However, it was found that the pure *trans*-isomers **6aA**, **6eA** and **6pA** are able to form tricyclic systems of cyclopenta[*b*]furo[2,3-*c*]pyrrole 7 in the RRM reaction (the last column of Tables 2 and 4). Moreover, in contrast to the communications [9–11,17,19,21,22], in our case, the ring-rearrangement metathesis does not require the supporting application of ethylene that facilitates practical synthesis.

Table 4. Optimization of the RRM protocol using the test esters **6eA** and **6pA**.

Entry	Starting Ester	Catalyst (mol %)	Conditions	Target Tricycle	Yield, % ^a
1	6eA	Cat. 1 (0.5)	CHCl ₃ , Δ, 3 h, Ar	7e	85
2	6eA	Cat. 1 (0.5)	CHCl ₃ , Δ, 1.5 h, Ar	7e	80
3	6eA	Cat. 1 (0.5)	CHCl ₃ , Δ, 1.0 h, Ar	7e	82
4	6eA	Cat. 1 (0.5)	CHCl ₃ , Δ, 0.5 h, Ar	7e	80^b
5	6eA	HG-II (0.5)	CHCl ₃ , Δ, 0.5 h, Ar	7e	74
6	6eA	Cat. 1 (0.5)	CHCl ₃ , Δ, 0.25 h, air	7e	35
7	6eA	Cat. 1 (0.5)	CHCl ₃ , Δ, 0.25 h, Ar	7e	83^b
8	6eA	Cat. 1 (0.5)	CH ₂ Cl ₂ , Δ, 3 h, Ar	7e	58
9	6eA	Cat. 1 (0.5)	CH ₂ Cl ₂ , Δ, 1.5 h, Ar	7e	52
10	6eA	Cat. 1 (0.5)	CH ₂ Cl ₂ , Δ, 0.5 h, Ar	7e	37
11	6eA	Cat. 1 (1.0)	CHCl ₃ , Δ, 0.25 h, Ar	7e	85
12	6eA	Cat. 1 (1.0)	CHCl ₃ , Δ, 0.5 h, Ar	7e	85
13	6eA	Cat. 1 (0.1)	CHCl ₃ , Δ, 0.25 h, Ar	7e	32
14	6eA	Cat. 1 (0.1)	CHCl ₃ , Δ, 1.0 h, Ar	7e	51
15	6eA	Cat. 1 (0.1)	CHCl ₃ , Δ, 1.5 h, Ar	7e	54
16	6eA	Cat. 1 (0.1)	CHCl ₃ , Δ, 3 h, Ar	7e	55
17	6pA	Cat. 2 (0.5)	CHCl ₃ , Δ, 30 min, Ar, MW, 120 °C	7p	55
18	6pA	Cat. 2 (0.5)	CHCl ₃ , Δ, 20 min, Ar, MW, 120 °C	7p	52
19	6pA	Cat. 2 (0.5)	CHCl ₃ , Δ, 10 min, Ar, MW, 120 °C	7p	45
20	6pA	Cat. 2 (0.5)	CH ₂ Cl ₂ , Δ, 30 min, Ar, MW, 120 °C	7p	85
21	6pA	Cat. 2 (0.5)	CH ₂ Cl ₂ , Δ, 20 min, Ar, MW, 120 °C	7p	84
22	6pA	Cat. 2 (0.5)	CH ₂ Cl ₂ , Δ, 15 min, Ar, MW, 120 °C	7p	80
23	6pA	Cat. 2 (0.5)	CH ₂ Cl ₂ , Δ, 10 min, Ar, MW, 100 °C	7p	0
24	6pA	Cat. 2 (0.5)	CH ₂ Cl ₂ , Δ, 10 min, Ar, MW, 120 °C	7p	82^b
25	6pA	HG-II (0.5)	CH ₂ Cl ₂ , Δ, 10 min, Ar, MW, 120 °C	7p	42
26	6pA	Cat. 2 (1.0)	CH ₂ Cl ₂ , Δ, 10 min, Ar, MW, 120 °C	7p	83
25	6pA	Cat. 2 (1.0)	CH ₂ Cl ₂ , Δ, 15 min, Ar, MW, 120 °C	7p	85
26	6pA	Cat. 2 (0.1)	CH ₂ Cl ₂ , Δ, 10 min, Ar, MW, 120 °C	7p	43
27	6pA	Cat. 2 (0.1)	CH ₂ Cl ₂ , Δ, 15 min, Ar, MW, 120 °C	7p	47

^a Isolated yields of products **7** after column chromatography. ^b In gray—the best conditions and yields (in bold) are highlighted.

To achieve the maximum yield of the target tricycles **7**, the metathesis reaction was optimized in terms of solvent, temperature, duration and amount of catalyst. Due to the poor solubility of esters **6eA** (3-allyl) and **6pA** (3-methylallyl) in benzene and *o*-dichlorobenzene, we chose not to use aromatic solvents; similarly, polar solvents such as THF or MeCN proved to be ineffective in view of their capacity to interact with the Hoveyda–Grubbs type catalysts at elevated temperatures. The best of the tested mediums turned out to be halogenomethanes (CH₂Cl₂ and CHCl₃), and hence they were used as solvents in all further experiments.

None of the selected catalysts exhibited activity at temperatures below 50 °C, and no rearrangement products **7e,p** were fixed. Being the most active, the morpholine containing **Cat. 1** started to work at the temperature of boiling chloroform (~60 °C), causing the rearrangement of the test 3-allyl isoindolone **6e**. The more sterically demanding methylallylic substrate **6pA** are not cyclized under these conditions. An increase in temperature up to 100 °C under microwave irradiation led to a rapid decomposition of **Cat. 1** (at 100 °C, the emerald-green color of the chloroform solution of **Cat. 1** turned brown almost immediately), and accordingly to low yields of the product **7p**. Obviously, higher temperatures and a more thermally stable catalyst should be used for a successful cyclization of methylallyl derivatives **6i–p**.

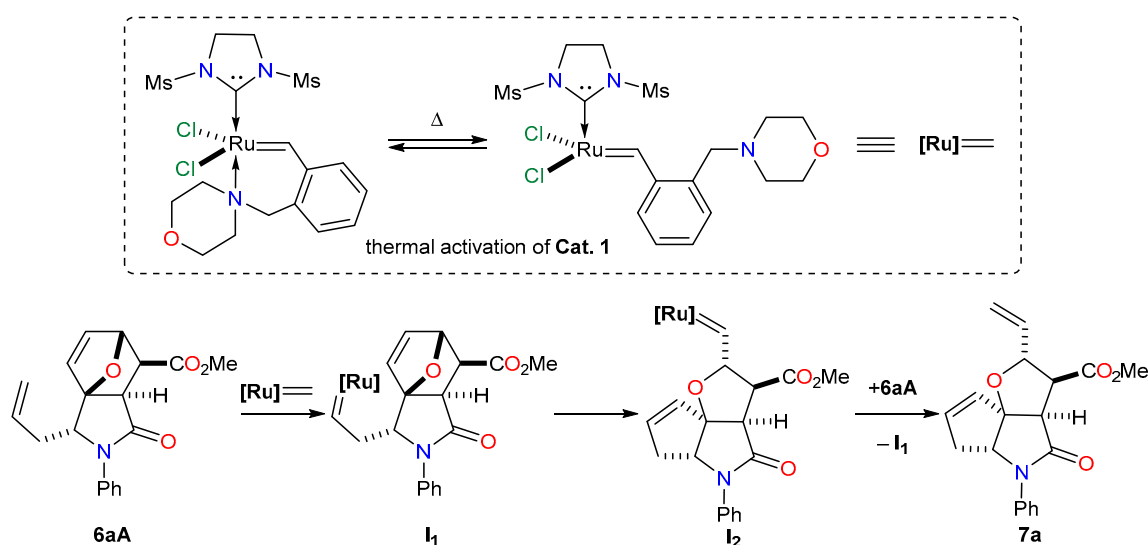
N,N-Dimethylamino derivative (**Cat. 2**), with a shorter bond length between nitrogen and ruthenium (the N→Ru bond is 2.24 Å [27]), is stable at least up to 140 °C [27], and therefore turned out to be effective for the preparation of cyclopenta[*b*]furo[2,3-*c*]pyrrole **7p** at temperatures above 100 °C in microwave-assisted experiments (entries 17–26, Table 4). It should be noted that the amount of catalysts **1** and **2** required for the complete conversion of the initial esters **6eA**, **6pA** did not exceed 0.5 mol % in both cases, while the reaction time was much shorter than in the papers cited above [9–23].

After all attempts, the following conditions were found to be optimal for the recyclizations of the allyl derivative (**6eA**): boiling chloroform, 0.5 mol % of **Cat. 1**, 30 min. For synthesis of the methyl substituted **6pA**, the best results were achieved under microwave activation in CH₂Cl₂ at 120 °C, 10 min, **Cat. 2** (0.5 mol %).

It was interesting to compare the potential of the commercially available HG-II catalyst with catalysts **Cat.1** and **Cat.2** (see entries 4, 5, 24 and 25 in light gray in Table 4). Analysis of the isolated yields of products **7e,p** allows us to conclude that the most popular commercial catalyst (HG-II) is less efficient.

The optimized protocols discussed above were planned to be extended to the recyclization of the remaining esters **6** (Table 2). However, the obvious disadvantage of the method is the need to separate mixtures of diastereomers **6A/6B**. We tried to get around this obstacle, taking into account that *cis*-isomers **6aB–6pB** can be considered as undesirable ballast in the target tricycles **7** synthesis, and that the proposed pathway is based on readily available starting materials and reliable synthetic procedures, which allows the synthesis to be scaled up to kilogram quantities. Thereby, the developed approaches were further applied to the metathesis of mixtures of isomers **6A/6B** (Scheme 5). To our satisfaction, the admixtures of *cis*-isomers **6B** had no significant impact on the reaction progress; the polymerization products formed from them could be easily separated during purification by flash or column chromatography to provide the pure cyclopenta[*b*]furo[2,3-*c*]pyrroles **7** in good yields (based on the *trans*-isomer **6A**). Thus, the majority of the RRM reactions presented in Table 2 were carried out using mixtures of isomers **6A/6B** as starting materials.

It worth mentioning here that by revising the ethylene-supported transformations of the similar substrates [9–23], the question of the sequence of metathesis stages arose. In theory, two paths exist for the rearrangement of **6** to **7** in an ethylene atmosphere: ROM/RCM, or vice versa, RCM/ROM successions [43]. We suppose that the plausible mechanism of the metathesis of *trans*-isomers **6A** does not differ from the generally accepted one, as it is represented in Scheme 7.

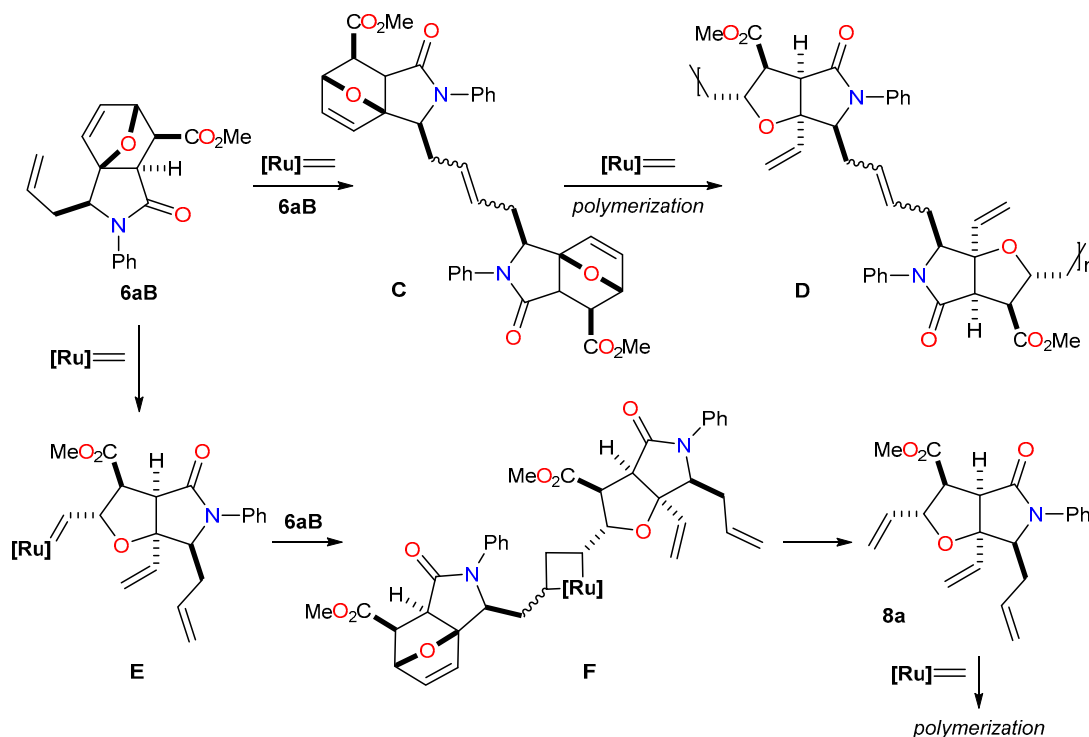


Scheme 7. Possible reaction sequence for RRM by the example of the conversion of *trans*-isomer **6aA** to **7a** in the presence of **Cat. 1**.

We did not set ourselves the goal of investigating in detail the reaction mechanism; however, from general considerations, it can be assumed that the ring-closing metathesis (RCM) stage has to precede the opening of the 7-oxabicycloheptene cycle (ROM). This statement is supported by the observed behavior of *trans*-3-allyl derivatives **6aA–6hA**, which regroup more quickly and under more mild conditions compared to their 3-methallyl analogs **6iA–6pA**. This fact is probably related to the more rapid cycloaddition of the double bond of the allylic fragment to the $Ru=CH-R$ center of the catalyst with the formation of structure **I₁** (Scheme 7). This statement is in good accordance with recently published data [43,44].

During the metathesis of *cis*-isomers **6B**, which are not capable of RCM, the polymer similar to **D** is apparently formed through the cross-metathesis intermediate **C** (Scheme 8). Although the *exo*-cyclic

allylic double bond is more reactive, it is also possible to obtain the short-lived triene **8a** which is generated in the course of the catalytic cleavage of the *endo*-cyclic double bond in the starting molecules **6B** (ruthenium complexes **E** and **F**).



Scheme 8. Possible behavior of *cis*-isomer **6aB** under metathesis reaction conditions.

3. Materials and Methods

3.1. General Remarks

All reagents were purchased from commercial suppliers (Acros Organics, Morris Plains, NJ, USA and Merck KGaA, Darmstadt, Germany) and used without further purification. Metathesis reactions required solvents (CH_2Cl_2 and CHCl_3) pre-dried over anhydrous P_2O_5 and an inert atmosphere (dry Ar). Thin layer chromatography was carried out on aluminum backed silica pre-coated plates «Sorbfil» and «Alugram». The plates were visualized using a water solution of KMnO_4 or UV (254 nm). After extraction, organic layers were dried over anhydrous MgSO_4 . IR spectra were obtained in KBr pellets or in thin films using an Infracum FT-801 IR-Fourier. NMR spectra were run in deuterated solvents (>99.5 atom % D) on Jeol JNM-ECA 600 (600.1 MHz for ^1H and 150.9 MHz for ^{13}C) spectrometer for 2–5% solutions in CDCl_3 or $\text{DMSO-}d_6$ at 22–23 °C using residual solvent signals (7.26/77.0 ppm for $^1\text{H}/^{13}\text{C}$ in CDCl_3 and 2.50/39.5 ppm for $^1\text{H}/^{13}\text{C}$ in $\text{DMSO-}d_6$) or TMS as an internal standard. CFCl_3 was used as an internal standard for ^{19}F -NMR spectra.

3.2. Experimental Procedures

The initial homoallylamines **4a–p** were synthesized according to the previously described procedures [45,46]. Carboxylic acids **5a–p** were synthesized using the known methods [29–32]. The detailed description of the preparation for all new compounds obtained in this work is given in the ESI section.

4. Conclusions

Our systematic studies on furan chemistry and metathesis reactions resulted in the development of general, effective method for the synthesis of natural product-like cyclopenta[*b*]furo[2,3-*c*]pyrroles from easily available, renewable furan-based precursors. The target tricyclic molecules were formed in high yields from esters of 3-allyl or 3-methallyl substituted 3a,6-epoxyisondolo-7-carboxylic acids in the presence of a new type of Hoveyda–Grubbs catalysts. The influence of the length of the N→Ru coordinate bond in the ruthenium complexes on the rate of the reaction was examined, and selective catalysts for the RRM of the allyl and methallyl derivatives were discovered. It was also proven that the recyclization is strictly stereoselective; only *trans*-isomer from two possible diastereoisomers of the initial methyl 3a,6-epoxyisondolo-7-carboxylates can be involved in the metathesis reaction.

Supplementary Materials: The following are available online, Figure S1: Structure of **6eA** (296 K) C₁₉H₁₈ClNO₄ (CCDC number 2023634), Figure S2: Structure of **6eB** (296 K) C₁₉H₁₈ClNO₄ (CCDC number 2023635), Figure S3: The overlay of molecules of *trans*-**6eA** (blue) and *cis*-**6eB** (red) methyl 3-allyl-2-(4-chlorophenyl)-1-oxo-1,2,3,6,7,7a-hexahydro-3a,6-epoxyisondolo-7-carboxylates according to the single crystal XRD, Figure S4: Structure of **8b** (CCDC number is 2025199), Table S1: Crystal data and structure refinement for **6eA** and **6eB**, Table S2: Bond Lengths for **6eA**, Table S3: Bond Angles for **6eA**, Table S4: Hydrogen Bonds for **6eA**, Table S5: Bond Lengths for **6eB**, Table S6: Bond Angles for **6eB**, Table S7: Hydrogen Bonds for **6eB**, Table S8: Crystal data and structure refinement for **8b**, Table S9: Bond Lengths for **8b**, Table S10: Bond Angles for **8b**, Table S11: Hydrogen Bonds for **8b**, Table S12: Selected ¹H-NMR chemical shifts for *trans*- and *cis*-isomers, Table S13: Selected ¹³C-NMR chemical shifts for *trans*- and *cis*-isomers.

Author Contributions: A.S.A., M.A.V., P.A.K., and N.L.M. performed the synthesis and purification of the obtained compounds; A.A.S. and M.S.G. performed the X-ray diffraction experiments; K.B.P. conducted the NMR data analysis; R.A.N. performed the NMR experiments; V.V.K. organized the drafts' preparation and participated in the editing; F.I.Z. conceived, designed the experiments and supervised all processes of this investigation. All authors have read and agreed to the published version of the manuscript.

Funding: The authors extend their appreciation to the Russian Science Foundation (RSF) for funding this work through a general research project under grant number (project No. 18-13-00456).

Conflicts of Interest: The authors declare no conflict of interest.

References

1. Ogba, O.M.; Warner, N.C.; O'Leary, D.J.; Grubbs, R.H. Recent advances in ruthenium-based olefin metathesis. *Chem. Soc. Rev.* **2018**, *47*, 4510–4544. [[CrossRef](#)]
2. Kotha, S.; Dipak, M.K. Strategies and tactics in olefin metathesis. *Tetrahedron* **2012**, *68*, 397–421. [[CrossRef](#)]
3. Hughes, D.; Wheeler, P.; Ene, D. Olefin Metathesis in Drug Discovery and Development- Examples from Recent Patent Literature. *Org. Process Res. Dev.* **2017**, *21*, 1938–1962. [[CrossRef](#)]
4. Higman, C.S.; Lummiss, J.A.; Fogg, D. Olefin Metathesis at the Dawn of Implementation in Pharmaceutical and Specialty-Chemicals Manufacturing. *Angew. Chem. Int. Ed.* **2016**, *55*, 3552–3565. [[CrossRef](#)]
5. Yu, M.; Lou, S.; Gonzalez-Bobes, F. Closing Metathesis in Pharmaceutical Development: Fundamentals, Applications, and Future Directions. *Org. Process Res. Dev.* **2018**, *22*, 918–946. [[CrossRef](#)]
6. Müller, D.S.; Baslé, O.; Mauduit, M.A. Tutorial review of stereoretentive olefin metathesis based on ruthenium dithiolate catalysts. *Beilstein J. Org. Chem.* **2018**, *14*, 2999–3010. [[CrossRef](#)]
7. Montgomery, T.P.; Johns, A.M.; Grubbs, R.H. Recent Advancements in Stereoselective Olefin Metathesis Using Ruthenium Catalysts. *Catalysts* **2017**, *7*, 87. [[CrossRef](#)]
8. Nolan, S.P.; Clavier, H. Chemoselective olefin metathesis transformations mediated by ruthenium complexes. *Chem. Soc. Rev.* **2010**, *39*, 3305–3316. [[CrossRef](#)]
9. Lam, J.K.; Schmidt, Y.; Vanderwal, C.D. Complex polycyclic scaffolds by metathesis rearrangement of Himbert arene/allene cycloadducts. *Org. Lett.* **2012**, *14*, 5566–5569. [[CrossRef](#)]
10. Kotha, S.; Meshram, M.; Khedkar, P.; Banerjee, S.; Deodhar, D. Recent applications of ring-rearrangement metathesis in organic synthesis. *Beilstein J. Org. Chem.* **2015**, *11*, 1833–1864. [[CrossRef](#)]
11. Kotha, S.; Pulletikurti, S.A. Metathetic Approach to [5/5/6] Aza-Tricyclic Core of Dendrobine, Kopsanone, and Lycopalhine A Type of Alkaloids. *Synthesis* **2019**, *51*, 3981–3988. [[CrossRef](#)]

12. Kotha, S.; Meshram, M.; Dommaraju, Y. Design and Synthesis of Polycycles, Heterocycles, and Macrocycles via Strategic Utilization of Ring-Closing Metathesis. *Chem. Rec.* **2018**, *18*, 1613–1632. [[CrossRef](#)] [[PubMed](#)]
13. Kiss, L.; Kardos, M.; Vass, C.; Fülöp, F. Application of metathesis reactions in the synthesis and transformations of functionalized beta-amino acid derivatives. *Synthesis* **2018**, *50*, 3571–3588. [[CrossRef](#)]
14. Acharyya, R.K.; Rej, R.K.; Nanda, S. Exploration of Ring Rearrangement Metathesis Reaction: A General and Flexible Approach for the Rapid Construction [5,n]-Fused Bicyclic Systems en Route to Linear Triquinanes. *J. Org. Chem.* **2018**, *83*, 2087–2103. [[CrossRef](#)] [[PubMed](#)]
15. Clavier, H.; Broggi, J.; Nolan, S.P. Ring-Rearrangement Metathesis (RRM) Mediated by Ruthenium-Indenylidene Complexes. *Eur. J. Org. Chem.* **2010**, *2010*, 937–943. [[CrossRef](#)]
16. Datta, R.; Ghosh, S. Domino ring-opening–ring-closing enyne metathesis vs. enyne metathesis of norbornene derivatives with alkynyl side chains. Construction of condensed polycarbocycles. *Beilstein J. Org. Chem.* **2018**, *14*, 2708–2714. [[CrossRef](#)]
17. Kotha, S.; Ravikumar, O. Design and synthesis of oxa-bowls via Diels–Alder reaction and ring-rearrangement metathesis as key steps. *Tetrahedron Lett.* **2014**, *55*, 5781–5784. [[CrossRef](#)]
18. Kotha, S.; Ravikumar, O. Ring-Rearrangement-Metathesis Approach to Polycycles: Substrate-Controlled Stereochemical Outcome During Grignard Addition. *Eur. J. Org. Chem.* **2016**, 3900–3906. [[CrossRef](#)]
19. Funel, J.A.; Prunet, J. Domino metathesis reactions for the synthesis of fused tricyclic frameworks. *Synlett* **2005**, 235–238. [[CrossRef](#)]
20. Kotha, S.; Ravikumar, O. Diversity–Oriented Approach to Carbocycles and Heterocycles through Ring–Rearrangement Metathesis, Fischer Indole Cyclization, and Diels–Alder Reaction as Key Steps. *Eur. J. Org. Chem.* **2014**, *2014*, 5582–5590. [[CrossRef](#)]
21. Kotha, S.; Pulletikurti, S. Synthesis of propellanes containing a bicyclo[2.2.2]octene unit via the Diels–Alder reaction and ring-closing metathesis as key steps. *RCS Adv.* **2018**, *8*, 14906–14915. [[CrossRef](#)]
22. Kotha, S.; Aswar, V.R. Target specific tactics in olefin metathesis: Synthetic approach to *cis-syn-cis*-triquinanes and propellanes. *Org. Lett.* **2016**, *18*, 1808–1811. [[CrossRef](#)] [[PubMed](#)]
23. Cheng-Sánchez, I.; Sarabia, F. Recent Advances in Total Synthesis via Metathesis Reactions. *Synthesis* **2018**, *50*, 3749–3786.
24. Firth, J.D.; Craven, P.G.E.; Lilburn, M.; Pahl, A.; Marsden, S.P.; Nelson, A. A biosynthesis-inspired approach to over twenty diverse natural product-like scaffolds. *Chem. Commun.* **2016**, *52*, 9837–9840. [[CrossRef](#)]
25. Mariscal, R.; Maireles-Torres, P.; Ojeda, M.; Sádaba, I.; Granados, M.L. Furfural: A renewable and versatile platform molecule for the synthesis of chemicals and fuels. *Energy Environ. Sci.* **2016**, *9*, 1144–1189. [[CrossRef](#)]
26. Bozell, J.J.; Petersen, G.R. Technology development for the production of biobased products from biorefinery carbohydrates—The US Department of Energy’s “Top 10” revisited. *Green Chem.* **2010**, *12*, 539–554. [[CrossRef](#)]
27. Polyanskii, K.B.; Alekseeva, K.A.; Raspertov, P.V.; Kumandin, P.A.; Nikitina, E.V.; Gurbanov, A.V.; Zubkov, F.I. Hoveyda–Grubbs catalysts with an N→Ru coordinate bond in a six-membered ring. Synthesis of stable, industrially scalable, highly efficient ruthenium metathesis catalysts and 2-vinylbenzylamine ligands as their precursors. *Beilstein J. Org. Chem.* **2019**, *15*, 769–779. [[CrossRef](#)]
28. Polyanskii, K.B.; Alekseeva, K.A.; Kumandin, P.A.; Atioğlu, Z.; Akkurt, M.; Toze, F.A. Crystal structure of [1,3-bis(2,4,6-trimethylphenyl)imidazolidin-2-ylidene]dichlorido[2-[1-(dimethylamino)ethyl]benzylidene] ruthenium including an unknown solvate. *Acta Cryst. E* **2019**, *75*, 342–345. [[CrossRef](#)]
29. Zubkov, F.I.; Boltukhina, E.V.; Turchin, K.F.; Borisov, R.S.; Varlamov, A.V. New synthetic approach to substituted isoindolo[2,1-*a*]quinoline carboxylic acids via intramolecular Diels–Alder reaction of 4-(N-furyl-2)-4-arylamino-butenes-1 with maleic anhydride. *Tetrahedron* **2005**, *61*, 4099–4113. [[CrossRef](#)]
30. Boltukhina, E.V.; Zubkov, F.I.; Nikitina, E.V.; Varlamov, A.V. Novel approach to isoindolo[2,1-*a*]quinolines: Synthesis of 1-and 3-halo-substituted 11-oxo-5,6,6a,11-tetrahydroisoindolo [2,1-*a*]quinoline-10-carboxylic acids. *Synthesis* **2005**, *2005*, 1859–1875. [[CrossRef](#)]
31. Zubkov, F.I.; Boltukhina, E.V.; Nikitina, E.V.; Varlamov, A.V. Study of regioselectivity of intramolecular cyclization of *N*-(*m*-R-phenyl)- and *N*-(α -naphthyl)-2-allyl(methallyl)-6-carboxy-4-oxo-3-aza-10-oxatricyclo[5.2.1.0^{1,5}]dec-8-enes. *Russ. Chem. Bull.* **2004**, *53*, 2816–2829. [[CrossRef](#)]
32. Varlamov, A.V.; Boltukhina, E.V.; Zubkov, F.I.; Nikitina, E.V.; Turchin, K.F. Intramolecular [4+2] cycloaddition of furfurylsubstituted homoallylamines to allylhalides, acryloyl chloride and maleic anhydride. *J. Heterocyclic Chem.* **2006**, *43*, 1479–1495. [[CrossRef](#)]

33. Zubkov, F.I.; Nikitina, E.V.; Varlamov, A.V. Thermal and catalytic intramolecular [4+2]-cycloaddition in 2-alkenylfurans. *Russ. Chem. Rev.* **2005**, *74*, 639–669. [[CrossRef](#)]
34. Padwa, A.; Flick, A.C. Intramolecular Diels–Alder Cycloaddition of Furans (IMDAF) for Natural Product Synthesis. *Adv. Heterocycl. Chem.* **2013**, *110*, 1–41.
35. Kiselev, V.D.; Kornilov, D.A.; Sedov, I.A.; Konovalov, A.I. Solvent Influence on the Diels–Alder Reaction Rates of 9-(Hydroxymethyl)anthracene and 9,10-Bis(hydroxymethyl)anthracene with Two Maleimides. *Int. J. Chem. Kinet.* **2017**, *49*, 61–68. [[CrossRef](#)]
36. Widstrom, A.L.; Lear, B.J. Structural and solvent control over activation parameters for a pair of retro Diels–Alder reactions. *Sci. Rep.* **2019**, *9*, 18267. [[CrossRef](#)]
37. Gandini, A.; Coelho, D.; Silvestre, A.J. Reversible click chemistry at the service of macromolecular materials. Part 1: Kinetics of the Diels–Alder reaction applied to furan–maleimide model compounds and linear polymerizations. *Eur. Polym. J.* **2008**, *44*, 4029–4036. [[CrossRef](#)]
38. Kotha, S.; Banerjee, S. Recent developments in the retro-Diels–Alder reaction. *RSC Adv.* **2013**, *3*, 7642–7666. [[CrossRef](#)]
39. Pedrosa, R.; Andrés, C.; Nieto, J. A short diastereoselective synthesis of enantiopure highly substituted tetrahydroepoxyisoindolines. *J. Org. Chem.* **2000**, *65*, 831–839. [[CrossRef](#)]
40. Zubkov, F.I.; Boltukhina, E.V.; Turchin, K.F.; Varlamov, A.V. An efficient approach to isoindolo [2,1-*b*][2] benzazepines via intramolecular [4+2] cycloaddition of maleic anhydride to 4- α -furyl-4-N-benzylaminobut-1-enes. *Tetrahedron* **2004**, *60*, 8455–8463. [[CrossRef](#)]
41. Pedrosa, R.; Sayalero, S.; Vicente, M.; Casado, B. Chiral Template Mediated Diastereoselective Intramolecular Diels–Alder Reaction Using Furan as a Diene. Toward the Synthesis of Enantiopure Trisubstituted Tetrahydroepoxyisoindolones. *J. Org. Chem.* **2005**, *70*, 7273–7278. [[CrossRef](#)] [[PubMed](#)]
42. Suzuki, M.; Okada, T.; Taguchi, T.; Hanzawa, Y.; Iitaka, Y. Intramolecular Diels–Alder reactions of furan derivatives: Steric and electronic effects of trifluoromethyl groups. *J. Fluorine Chem.* **1992**, *57*, 239–243. [[CrossRef](#)]
43. Holub, N.; Blechert, S. Ring-Rearrangement Metathesis. *Chem. Asian J.* **2007**, *2*, 1064–1082. [[CrossRef](#)] [[PubMed](#)]
44. Harrity, J.P.; Visser, M.S.; Gleason, J.D.; Hoveyda, A.H. Ru-Catalyzed Rearrangement of Styrenyl Ethers. Enantioselective Synthesis of Chromenes through Zr- and Ru-Catalyzed Processes. *J. Am. Chem. Soc.* **1997**, *119*, 1488–1489. [[CrossRef](#)]
45. Kouznetsov, V.; Öcal, N.; Turgut, Z.; Zubkov, F.; Kaban, S.; Varlamov, A. Allylation and Heterocycloaddition reactions of Aldimines: Furan- and Quinolinecarboxaldehydes. *Monatsh. Chem.* **1998**, *129*, 671–677. [[CrossRef](#)]
46. Urbina, J.M.; Cortés, J.C.; Palma, A.; López, S.N.; Zacchino, S.A.; Enriz, R.D.; Ribas, C.; Kouznetsov, V.V. Inhibitors of the fungal cell wall. Synthesis of 4-aryl-4-N-arylamine-1-butenes and related compounds with inhibitory activities on β (1–3) glucan and chitin synthases. *Bioorg. Med. Chem.* **2000**, *8*, 691–698. [[CrossRef](#)]

Sample Availability: Samples of the compounds 5–7 are available from the authors.

Publisher’s Note: MDPI stays neutral with regard to jurisdictional claims in published maps and institutional affiliations.



© 2020 by the authors. Licensee MDPI, Basel, Switzerland. This article is an open access article distributed under the terms and conditions of the Creative Commons Attribution (CC BY) license (<http://creativecommons.org/licenses/by/4.0/>).